



# HHS Public Access

Author manuscript

*J Biomed Mater Res B Appl Biomater.* Author manuscript; available in PMC 2015 October 01.

Published in final edited form as:

*J Biomed Mater Res B Appl Biomater.* 2015 July ; 103(5): 1044–1049. doi:10.1002/jbm.b.33290.

## Incorporation of copper into chitosan scaffolds promotes bone regeneration in rat calvarial defects

Sheetal D'Mello<sup>a</sup>, Satheesh Elangovan<sup>b,\*</sup>, Liu Hong<sup>c</sup>, Ryan D. Ross<sup>d</sup>, D. Rick Sumner<sup>d</sup>, and Aliasger K. Salem<sup>a,b,\*</sup>

<sup>a</sup>Division of Pharmaceutics and Translational Therapeutics, College of Pharmacy, University of Iowa, IA, 52242

<sup>b</sup>Department of Periodontics, College of Dentistry, University of Iowa, Iowa City, IA, 52242

<sup>b</sup>Department of Prosthodontics, University of Iowa College of Dentistry, Iowa City, IA, USA

<sup>d</sup>Department of Anatomy and Cell Biology, Rush Medical College, Chicago, IL, USA

### Abstract

The objective of this study was to investigate the effects of a copper loaded chitosan scaffold on bone regeneration in critical-sized calvarial defects in rats. Chitosan scaffolds and copper-chitosan scaffolds were fabricated and characterized by scanning electron microscopy (SEM). Chitosan and copper-chitosan scaffolds were implanted into 5 mm diameter critical-sized calvarial defects in Fisher 344 male rats. Empty defects (no scaffolds) were included as a control. After 4 weeks, the rats were sacrificed for micro-computed tomography (micro-CT) and histological analysis of new bone tissue development. Microscopy images revealed the uniformly porous structure of chitosan and copper-chitosan scaffolds. Significant bone regeneration was noted in the defects treated with copper-chitosan scaffolds when evaluated using micro-CT and histological analysis, when compared to other groups tested. On analysis of the micro-CT scans, an eleven-fold and a two-fold increase in the new bone volume/total volume (BV/TV) % was found in defects treated with the copper-chitosan scaffolds, when compared to empty defects and chitosan scaffolds, respectively. This study demonstrated the suitability of copper-crosslinked chitosan scaffolds for bone tissue engineering and provides the first evidence that inclusion of copper ions in scaffolds can enhance tissue regeneration.

### Keywords

Chitosan; Copper; Biodegradable scaffolds; Tissue engineering; Bone regeneration

\*Corresponding Authors: Dr. Aliasger K. Salem, 115 S. Grand Avenue, S228 PHAR, University of Iowa College of Pharmacy, Iowa City, IA 52242. aliasger-salem@uiowa.edu, Telephone: 319 335 8810, Fax: 319 335 9349, Dr. Satheesh Elangovan, 801 Newton Road, S464, Department of Periodontics, University of Iowa College of Dentistry, Iowa City, Iowa -52242, satheesh-elangovan@uiowa.edu, Telephone: 319 335 7543, Fax: 319 335 7239.

We have no conflicts of interest to declare.

## 1. Introduction

Bone defects resulting from tumor resection, periodontal disease, skeletal deficiency/disorder, abnormal development, and trauma, present significant health risks and are challenging to treat. Various approaches have been undertaken to treat bone defects with the goal of regenerating the lost osseous tissue thereby regaining function. Current treatments to treat bone defects are only partially effective and are often accompanied by major drawbacks such as limited supply and transplant rejection/incompatibility along with surgical side effects from harvesting bone such as infection, disease transmission or neurovascular injury.<sup>1-4</sup> Limitations of the current strategies of bone regeneration or replacement have led to tissue engineering approaches for repairing skeletal defects.<sup>5-7</sup> In orthopedics and dentistry, guided bone regeneration in combination with osteoconductive scaffolds is an alternative.<sup>8-10</sup> As such, there is a great need for biomaterials with higher bone regenerative capacity and predictability that favors complete bone regeneration without the aforementioned drawbacks.

Chitosan is an abundantly available natural biopolymer; it is biodegradable and biocompatible.<sup>11,12</sup> It undergoes enzymatic degradation to glucosamine, and N-acetylglucosamine copolymers, substances naturally found in the body which are excreted or used in the amino sugar pool.<sup>13</sup> Chitosan aids in hemostasis and plays a role in activation of macrophages and cytokine stimulation.<sup>13</sup> Chitosan has also been reported to induce collagen synthesis and angiogenesis in the early wound healing and tissue remodeling phases of wound repair.<sup>14,15</sup> Owing to these attributes, chitosan has generated significant interest as a biomaterial for a broad range of wound healing applications.<sup>16-18</sup> It has been shown that chitosan forms a chelate complex with metal ions and that copper ions strongly interact with chitosan.<sup>19,20</sup> The chelation between chitosan and copper ions that occurs through the four nitrogen ligands in a square-planar geometrical manner is responsible for the formation of tightly packed chitosan gel.<sup>21,22</sup>

Apart from the known physiological roles of copper in enzymatic reactions and protein functions, it has also been reported to act as an endogenous stimulator of angiogenesis by inducing the migration and proliferation of endothelial cells.<sup>23-25</sup> Copper has been demonstrated to induce vascular endothelial growth factor (VEGF) expression *in vitro* and *in vivo*.<sup>26</sup> The quality of regenerating tissue was also shown to be distinctly improved with a high density of cells in the granulation layer of copper-treated wounds. Copper-sensitive pathways are implicated to be involved in the regulation of key mediators of wound healing such as angiogenesis and tissue extracellular matrix remodeling. The primary objective of this proof of concept study is to develop chitosan scaffolds complexed with copper and test its *in vivo* bone regeneration capacity. This study, to our knowledge, is the first to develop and investigate the effect of copper crosslinked chitosan scaffold on bone tissue engineering in critical-sized calvarial defects.

## 2. Materials and methods

### 2.1. Materials

Chitosan (high purity,  $M_v$  110,000-150,000) and copper (II) sulfate were purchased from Sigma–Aldrich® (St. Louis, MO). All other chemicals and solvents used were of reagent grade.

### 2.2. Scaffold fabrication

To prepare the chitosan sponges, chitosan was dissolved in 0.3 M acetate buffer, pH 4.5 at a concentration of 2 % w/v and freeze-dried. The copper-chitosan scaffolds were prepared by slowly adding 450  $\mu$ l 2 % w/v chitosan solution to 50  $\mu$ l 0.625 mM copper solution in acetate buffer. The mixture was vortexed for 30 s-1 min for homogeneity, incubated at room temperature for 4 h and later freeze-dried to completely remove the solvent (Fig. 1). Addition of chitosan solution to the copper solution led to the spontaneous formation of chitosan gel without any leakage.

### 2.3. Morphological characterization of the scaffolds

Standard protocol for scanning electron microscopy (SEM, Hitachi Model S-4800, Japan) was employed. Briefly, the scaffolds were mounted on aluminum stubs, sputter-coated with gold and examined using the microscope operated at 3 kV accelerating voltage and a current of 10  $\mu$ A. The surface characteristics of the scaffolds, including pore interconnectivity and scaffold integrity were analyzed.

### 2.4. Surgical procedure: In vivo implantation of scaffolds

Inbred 14 week-old male Fisher (CDF®) white rats (F344/DuCrI, ~250 g) were obtained from Charles River Laboratories International, Inc (Wilmington, MA) and housed and cared in the animal facilities. The surgical procedures were approved by and performed according to guidelines established by the University of Iowa Institutional Animal Care and Use Committee, Iowa. The animals were anaesthetized by intra-peritoneal injection of ketamine (80 mg/kg)-xylazine (8 mg/kg) mixture (provided by the Office of Animal Resources, University of Iowa). A sagittal incision, ~1.5 – 2 cm, was made on the scalp of each rat, and the calvaria was exposed by blunt dissection. Two 5 mm diameter  $\times$  2 mm thickness critical-sized defects were generated using a round carbide bur on the parietal bone, on both sides of the sagittal suture. The defects were randomly allocated into the following study groups: (1) empty defect (n = 3); (2) chitosan scaffold (n = 2); and (3) copper-loaded chitosan scaffold (n = 2). The shape and size of the cylindrical scaffold discs was adjusted to fit into the defects with a diameter of 5 mm and a thickness of 2 mm and implanted into the rats. The incision was closed in layers using sterile silk sutures. Buprenorphine (0.15 mg, intramuscular), as an analgesic, was administered to each rat thereafter and the animals were carefully monitored during post-operative recovery. The rats were able to function normally after this procedure. After 4 weeks, all the animals were euthanized and the bony segments containing the regions of interest were harvested from the calvarial bone and fixed in 10 % neutral buffered formalin.

## 2.5. Micro-CT analysis

Three-dimensional microfocus x-ray microcomputed tomography imaging was performed on the specimens using a cone-beam micro-CT system (micro-CT40, Scanco Medical AG, Switzerland). Specimens were scanned in 70 % ethanol at 55 kVp and 145  $\mu$ A with a voxel size of 10  $\mu$ m and an integration time of 300 ms. Analysis was performed using a constant 5 mm diameter circular region of interest that was placed in the center of the machined defect and spanned a total of 50 reconstructed slices, such that a total cylindrical volume of interest of  $\sim$ 9.8 mm<sup>3</sup> oriented perpendicular to the outer table of the calvarium was analyzed for each specimen using the manufacturer's software (sigma = 0.8, support = 1.0, and threshold = 250). Bone volume (BV) per total volume (TV) in the bone defect was obtained.

## 2.6. Histological analysis of rat bone defects

The bone samples underwent a decalcification (Surgipath, Decalcifier II) procedure. When the decalcification end point test returned negative for the presence of calcium, the rat bone specimens were introduced into a paraffin processor for paraffin processing, paraffin embedded and the blocks were sectioned in the sagittal plane for each specimen. Histological analysis was performed on the 5  $\mu$ m sections in the central portion of the wound. The sections were collected on Superfrost Plus Slides (Fisher Scientific®), deparaffinized and stained with Harris hematoxylin and eosin (H & E staining) according to standard protocols. Sections representing the central area of each defect were used to observe the presence of collagen, new bone formation, and cells in order to evaluate bone regeneration after 4 weeks *in vivo* implantation. The bright field examination of the slides was done with an Olympus Stereoscope SZX12 and an Olympus BX61 microscope, both equipped with a digital camera.

## 2.7. Data presentation

Numerical data were reported as means with bars representing standard error of the mean (SEM) from replicate samples. Graphs were generated using Prism 5.0 (GraphPad Software Inc., San Diego, CA). The data was compared by ANOVA followed by a Tukey post-test analysis. The differences between the groups were considered to be statistically significant when the *P* value was < 0.05. Statistical analyses were performed using Prism 5.0 software.

## 3. Results and discussion

### 3.1. SEM analysis of chitosan scaffolds and chitosan-copper scaffolds

The three-dimensional porous polymer scaffold design creates and maintains a three-dimensional space within the defect *in vivo* for tissue regeneration. This facilitates the recruitment of healthy bone cells and other appropriate cell types from the surrounding tissue to the wound site, favors cellular attachment, and promotes the growth and differentiation of these cells. Subsequently, as a result, a space-filling tissue is formed over time as a result of cell localization facilitated by the scaffold.<sup>27</sup> Thus, within the defect, the three-dimensional scaffolds help control the size and shape of the regenerated, functional bone tissue. The crosslinking and gelation of polymeric chitosan chains induced by copper

(II) ions may also improve the mechanical strength and degradation rate of these scaffold matrices.

The freeze-drying technique was utilized in the preparation of scaffolds to obtain a three-dimensional structure with a spongy texture. In this method, the frozen solvent was removed by sublimation, and the now empty spaces once occupied by the frozen solvent crystals turned into the pores of the scaffold. The chitosan scaffolds showed a highly porous interconnecting network, with pore sizes of  $104 \pm 5 \mu\text{m}$  (Fig. 2a). The incorporation of copper within the scaffolds did not appear to have any adverse effect on the morphology or the micro-structural aspects of the final scaffold (Fig. 2b).

### 3.2. In vivo bone regeneration: Micro-CT scans

The chitosan scaffold matrix containing copper was evaluated *in vivo* for its efficacy as a bone regenerative biomaterial. Critical-sized calvarial defects were created in rats and were utilized as a model to test the *in vivo* efficacy of three different treatment groups: (1) empty defect (untreated) as a control, (2) defect filled with chitosan scaffold, and (3) defect filled with copper entrapped in the chitosan scaffold. The rats were sacrificed after 4 weeks and newly-formed bone tissue was evaluated for its volume using micro-CT scans. The micro-CT scan imaged the induced circular bone defects and the regenerated bone tissue in the defects as a result of various treatments (Fig. 3a–c, the circles superimposed on each of the representative images indicate the original bone defect edges). The empty, untreated defect displayed minimal irregular, patchy bone formation, while the chitosan scaffold exhibited much more organized mineralized regions towards the defect edge. In contrast, the scaffolds incorporating copper demonstrated remarkable mineralized tissue formation within the defect area, when compared to the other groups evaluated. The new bone tissue also appeared to be synthesized more towards periphery of the defect, and patterning to close in on the defect. This treatment was observed to have more hard tissue ingrowth from the edges of the defect within the implant region compared to empty defect and chitosan scaffold. The addition of chitosan solution to the copper sulfate solution results in the chelation of copper (II) ions with the amino groups of chitosan. This causes the gelation of chitosan solution and the retention of the copper (II) ions within the gel as well as the subsequent freeze-dried scaffolds.<sup>21</sup> We hypothesize that the presence of copper in the scaffold matrix may have accelerated the proliferation of epithelial and endothelial cells.<sup>28</sup> These functions, together with growth factor signaling, could have then promoted regeneration of the osseous tissue.<sup>29–31</sup>

### 3.3. In vivo bone regeneration: new bone volume fraction

The amount of bone tissue regenerated was quantified by analyzing bone volume fraction of the total tissue volume of interest – bone volume / total volume (BV/TV). The BV/TV was two-fold and eleven-fold higher in defects treated with copper-embedded chitosan scaffolds, when compared to the chitosan scaffold and empty defect control groups, respectively (Fig. 3d). Results of the ANOVA test provided evidence that the distribution of BV/TV outcomes differed significantly among the three treatment groups ( $p = 0.0418$ ). These highly macroporous scaffolds most likely, caused the cells in the vicinity to migrate into the scaffold and through its pores. The walls of the porous matrix act as a support for the attachment and

anchoring of cells. Since the pores are bigger in size than the cells, there is sufficient room within the scaffolds for tissue development. This structure facilitates the processes of cell growth and proliferation, differentiation, and angiogenesis, thereby enhancing local tissue repair.<sup>32</sup> The chitosan biomaterial surface together with copper may possibly be osteoconductive for progenitors and give rise to such processes. In addition, the incorporation of copper may have allowed for more cells to enter the scaffold through angiogenesis. Later, as the chitosan matrix biodegrades away, it is replaced by the newly-formed bone tissue.

#### 3.4. In vivo bone regeneration: H & E staining

Histology further confirmed the differences observed with micro-CT analysis. The pattern of distribution of mineralization across the defect regions as a result of different treatments observed in micro-CT images is consistent with histological examination using H & E stains. The image from the untreated, open defect showed that the defect created between the old bone edges was unfilled, while the chitosan scaffold group demonstrated more bone formation in the defect peripheries than empty defects (Fig. 4a–b). In the defect implanted with chitosan-copper scaffolds, we found significantly more bone formation in the defect than the other two groups. The bone formation is pronounced in the edges of the defects gradually protruding towards the center of the defect (Fig. 4c). The histology data demonstrated that the cells begin to regenerate the tissue and mineralization begins to occur around 4 weeks *in vivo*. We hypothesize that the copper is released gradually from the degrading chitosan matrix, which then results in endothelial cell proliferation leading to new blood vessel growth and osteoprogenitor recruitment into the scaffold. Copper has been studied to stimulate cell growth and division, and angiogenesis.<sup>23,24</sup> Along with oxygen and nutrients, new blood vessels help in the transportation of inflammatory cells and osteoprogenitors to the wound site, thus accelerating/improving bone healing, repair and regeneration.<sup>33</sup>

To our knowledge, this is the first report to explore the effect of adding copper (II) ions to scaffolds to enhance bone tissue regeneration. This proof of concept experiment clearly demonstrates the safety, feasibility and efficacy of chitosan copper scaffolds (relative to the controls or chitosan scaffolds) for bone tissue engineering. No biologics were employed in this study to make this scaffold osteoinductive and we relied completely on the osteoconductivity of the scaffold. In more comprehensive future studies, it will be necessary to carry out detailed physicochemical characterizations of the chitosan scaffolds with and without copper, determine if using higher concentrations of copper in the scaffolds generates any toxicity, quantify the degree of vascularization that occurs using chitosan copper scaffolds versus chitosan scaffolds alone and determine the kinetics of bone regeneration over time using chitosan scaffolds with and without copper. We anticipate that in future studies, this scaffold could promote complete bone regeneration when the experiments are extended to more than 4 weeks and potentially synergistic morphogens such as bone morphogenetic proteins (BMPs) are simultaneously incorporated into the scaffold.



## 4. Conclusions

Our results demonstrated that the copper-loaded chitosan scaffolds promoted osseous defect healing in calvarial defects in rats. This study demonstrated the feasibility and capability of copper-loaded chitosan scaffolds in enhancing the bone repair and regeneration process. These scaffolds, in combination with tissue inductive/conductive growth factors may be utilized for several biomedical applications including hard bone formation and soft tissue engineering.

## Acknowledgements

This study is supported by the University of Iowa Start-up Grant, the ITI Foundation for the Promotion of Implantology, Switzerland (ITI Research Grant No. 855 2012), the Osteology Foundation, Switzerland, the Osseointegration Foundation, USA, the American Cancer Society (RSG-09-015-01-CDD), and the National Cancer Institute at the National Institutes of Health (1R21CA13345-01/R21CA128414-01A2/UI Mayo Clinic Lymphoma SPORE) and the Lyle and Sharon Bighley Professorship. Rush University Medical Center MicroCT/Histology Core resources were used. Imaging equipment at the University of Iowa Core Microscopy Research Facility was used.

## References

1. Connolly JF, Guse R, Tiedeman J, Dehne R. Autologous marrow injection for delayed unions of the tibia: a preliminary report. *Journal of orthopaedic trauma*. 1989; 3(4):276–282. [PubMed: 2600692]
2. Lane JM, Tomin E, Bostrom MP. Biosynthetic bone grafting. *Clinical orthopaedics and related research*. 1999; 367:S107–S117. [PubMed: 10546640]
3. Petite H, Viateau V, Bensaid W, Meunier A, de Pollak C, Bourguignon M, Oudina K, Sedel L, Guillemin G. Tissue-engineered bone regeneration. *Nature biotechnology*. 2000; 18(9):959–963.
4. Vacanti CA, Upton J. Tissue-engineered morphogenesis of cartilage and bone by means of cell transplantation using synthetic biodegradable polymer matrices. *Clinics in plastic surgery*. 1994; 21(3):445–462. [PubMed: 7924143]
5. Jégoux F, Goyenvallé E, Cognet R, Malard O, Moreau F, Daculsi G, Aguado E. Reconstruction of irradiated bone segmental defects with a biomaterial associating MBCP+<sup>®</sup>, microstructured collagen membrane and total bone marrow grafting: An experimental study in rabbits. *Journal of Biomedical Materials Research Part A*. 2009; 91A(4):1160–1169. [PubMed: 19148925]
6. Lim H-C, Sohn J-Y, Park J-C, Um Y-J, Jung U-W, Kim C-S, Lee Y-K, Choi S-H. Osteoconductive effects of calcium phosphate glass cement grafts in rabbit calvarial defects. *Journal of Biomedical Materials Research Part B: Applied Biomaterials*. 2010; 95B(1):47–52.
7. Yaszemski MJ, Payne RG, Hayes WC, Langer R, Mikos AG. Evolution of bone transplantation: molecular, cellular and tissue strategies to engineer human bone. *Biomaterials*. 1996; 17(2):175–185. [PubMed: 8624394]
8. Aaboe M, Pinholt E, Hjørtting-Hansen E. Healing of experimentally created defects: a review. *British Journal of Oral and Maxillofacial Surgery*. 1995; 33(5):312–318. [PubMed: 8555150]
9. Hermann J, Buser D. Guided bone regeneration for dental implants. *Current opinion in periodontology*. 1995; 3:168–177. [PubMed: 8624562]
10. Yang C, Unursaikhan O, Lee J-S, Jung U-W, Kim C-S, Choi S-H. Osteoconductivity and biodegradation of synthetic bone substitutes with different tricalcium phosphate contents in rabbits. *Journal of Biomedical Materials Research Part B: Applied Biomaterials*. 2014; 102(1):80–88.
11. VandeVord PJ, Matthew HWT, DeSilva SP, Mayton L, Wu B, Wooley PH. Evaluation of the biocompatibility of a chitosan scaffold in mice. *Journal of Biomedical Materials Research*. 2002; 59(3):585–590. [PubMed: 11774317]
12. Wongrakpanich A, Adamcakova-Dodd A, Xie W, Joshi VB, Mapuskar KA, Geary SM, Spitz DR, Thorne PS, Salem AK. The Absence of CpG in Plasmid DNA-Chitosan Polyplexes Enhances Transfection Efficiencies and Reduces Inflammatory Responses in Murine Lungs. *Mol Pharm*. 2014

13. Baldrick P. The safety of chitosan as a pharmaceutical excipient. *Regul Toxicol Pharmacol.* 2010; 56(3):290–299. [PubMed: 19788905]
14. Azad AK, Sermsintham N, Chandkrachang S, Stevens WF. Chitosan membrane as a wound-healing dressing: Characterization and clinical application. *Journal of Biomedical Materials Research Part B: Applied Biomaterials.* 2004; 69B(2):216–222.
15. Kojima K, Okamoto Y, Miyatake K, Fujise H, Shigemasa Y, Minami S. Effects of chitin and chitosan on collagen synthesis in wound healing. *The Journal of veterinary medical science/the Japanese Society of Veterinary Science.* 2004; 66(12):1595–1598. [PubMed: 15644615]
16. Chandry T, Sharma CP. Chitosan-as a biomaterial. *Artificial Cells, Blood Substitutes and Biotechnology.* 1990; 18(1):1–24.
17. Muzzarelli R, Baldassarre V, Conti F, Ferrara P, Biagini G, Gazzanelli G, Vasi V. Biological activity of chitosan: ultrastructural study. *Biomaterials.* 1988; 9(3):247–252. [PubMed: 3408796]
18. Wang X, Ma J, Wang Y, He B. Bone repair in radii and tibias of rabbits with phosphorylated chitosan reinforced calcium phosphate cements. *Biomaterials.* 2002; 23(21):4167–4176. [PubMed: 12194519]
19. Rhazi M, Desbrieres J, Tolaimate A, Rinaudo M, Vottero P, Alagui A, El Meray M. Influence of the nature of the metal ions on the complexation with chitosan.: Application to the treatment of liquid waste. *European Polymer Journal.* 2002; 38(8):1523–1530.
20. Worthington KL, Adamcakova-Dodd A, Wongrakpanich A, Mudunkotuwa IA, Mapuskar KA, Joshi VB, Allan Guymon C, Spitz DR, Grassian VH, Thorne PS, Salem AK. Chitosan coating of copper nanoparticles reduces in vitro toxicity and increases inflammation in the lung. *Nanotechnology.* 2013; 24(39):395101. [PubMed: 24008224]
21. Kofuji K, Murata Y, Kawashima S. Sustained insulin release with biodegradation of chitosan gel beads prepared by copper ions. *International Journal of Pharmaceutics.* 2005; 303(1–2):95–103. [PubMed: 16139972]
22. Schlick S. Binding sites of copper<sup>2+</sup> in chitin and chitosan. An electron spin resonance study. *Macromolecules.* 1986; 19(1):192–195.
23. Hu GF. Copper stimulates proliferation of human endothelial cells under culture. *J Cell Biochem.* 1998; 69(3):326–335. [PubMed: 9581871]
24. McAuslan B, Reilly W. Endothelial cell phagokinesis in response to specific metal ions. *Experimental cell research.* 1980; 130(1):147–157. [PubMed: 6161014]
25. Raju KS, Alessandri G, Ziche M, Gullino PM. Ceruloplasmin, copper ions, and angiogenesis. *Journal of the National Cancer Institute.* 1982; 69(5):1183–1188. [PubMed: 6182332]
26. Sen CK, Khanna S, Venojarvi M, Trikha P, Ellison EC, Hunt TK, Roy S. Copper-induced vascular endothelial growth factor expression and wound healing. *American Journal of Physiology-Heart and Circulatory Physiology.* 2002; 282(5):H1821–H1827. [PubMed: 11959648]
27. Elangovan S, D'Mello SR, Hong L, Ross RD, Allamargot C, Dawson DV, Stanford CM, Johnson GK, Sumner DR, Salem AK. The enhancement of bone regeneration by gene activated matrix encoding for platelet derived growth factor. *Biomaterials.* 2014; 35(2):737–747. [PubMed: 24161167]
28. Borkow G. Copper's Role in Wound Healing. 2004
29. Heldin CH. Structural and functional studies on platelet-derived growth factor. *Embo j.* 1992; 11(12):4251–4259. [PubMed: 1425569]
30. Chang P-C, Seol Y-J, Cirelli JA, Pellegrini G, Jin Q, Franco LM, Goldstein SA, Chandler LA, Sosnowski B, Giannobile WV. PDGF-B gene therapy accelerates bone engineering and oral implant osseointegration. *Gene therapy.* 2010; 17(1):95–104. [PubMed: 19741730]
31. Bategay EJ, Rupp J, Iruela-Arispe L, Sage EH, Pech M. PDGF-BB modulates endothelial proliferation and angiogenesis in vitro via PDGF beta-receptors. *The Journal of cell biology.* 1994; 125(4):917–928. [PubMed: 7514607]
32. Wake MC, Patrick C Jr, Mikos A. Pore morphology effects on the fibrovascular tissue growth in porous polymer substrates. *Cell transplantation.* 1993; 3(4):339–343. [PubMed: 7522866]
33. Hankenson KD, Dishowitz M, Gray C, Schenker M. Angiogenesis in bone regeneration. *Injury.* 2011; 42(6):556–561. [PubMed: 21489534]



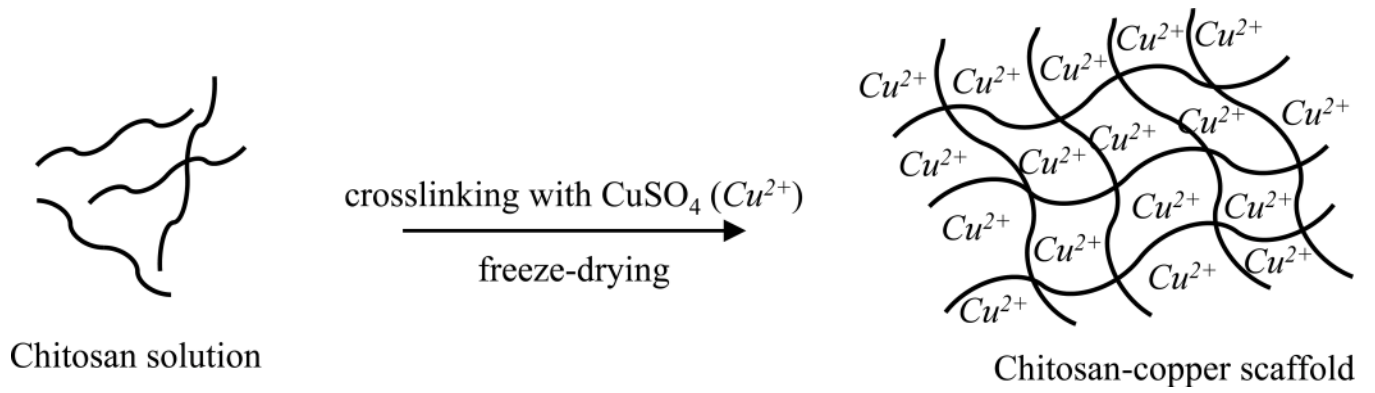


**Fig. 1.**  
Schematic showing the approach to preparing copper-chitosan scaffolds

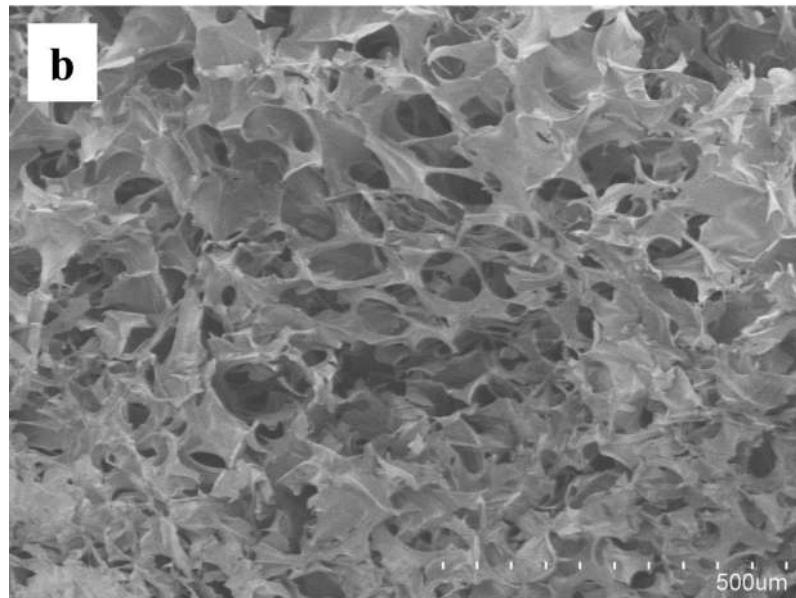
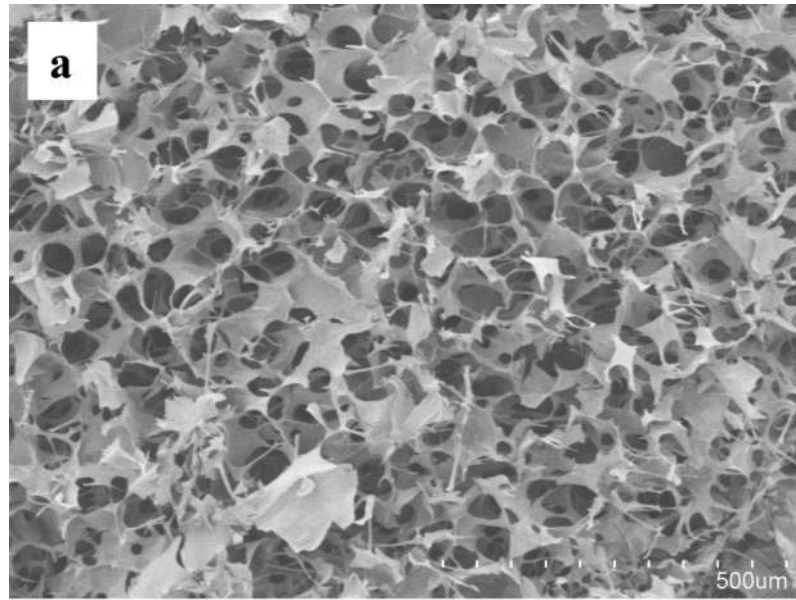


**Fig. 2.** SEM images of chitosan scaffolds (a) and chitosan scaffolds embedded with copper (b).

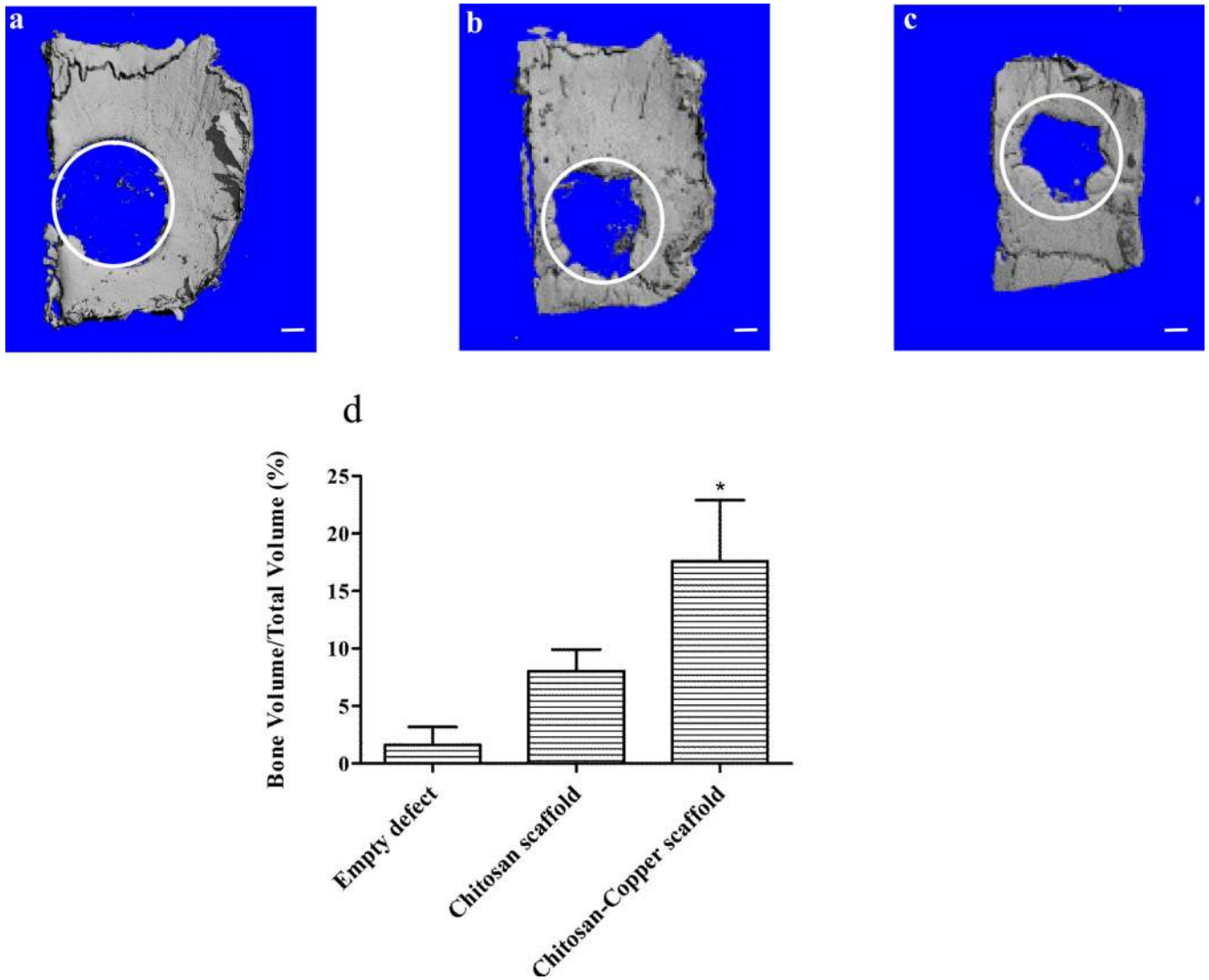


**Fig. 3.** Evaluation of *in vivo* bone formation: representative micro-CT scans showing the level of regenerated bone tissue after 4 weeks in empty defects (a, n = 3), chitosan scaffolds (b, n = 2) and copper-loaded chitosan scaffolds (c, n = 2). Assessment of regenerated bone volume fraction in defects treated with different groups (d). Scale bar, 1 mm.

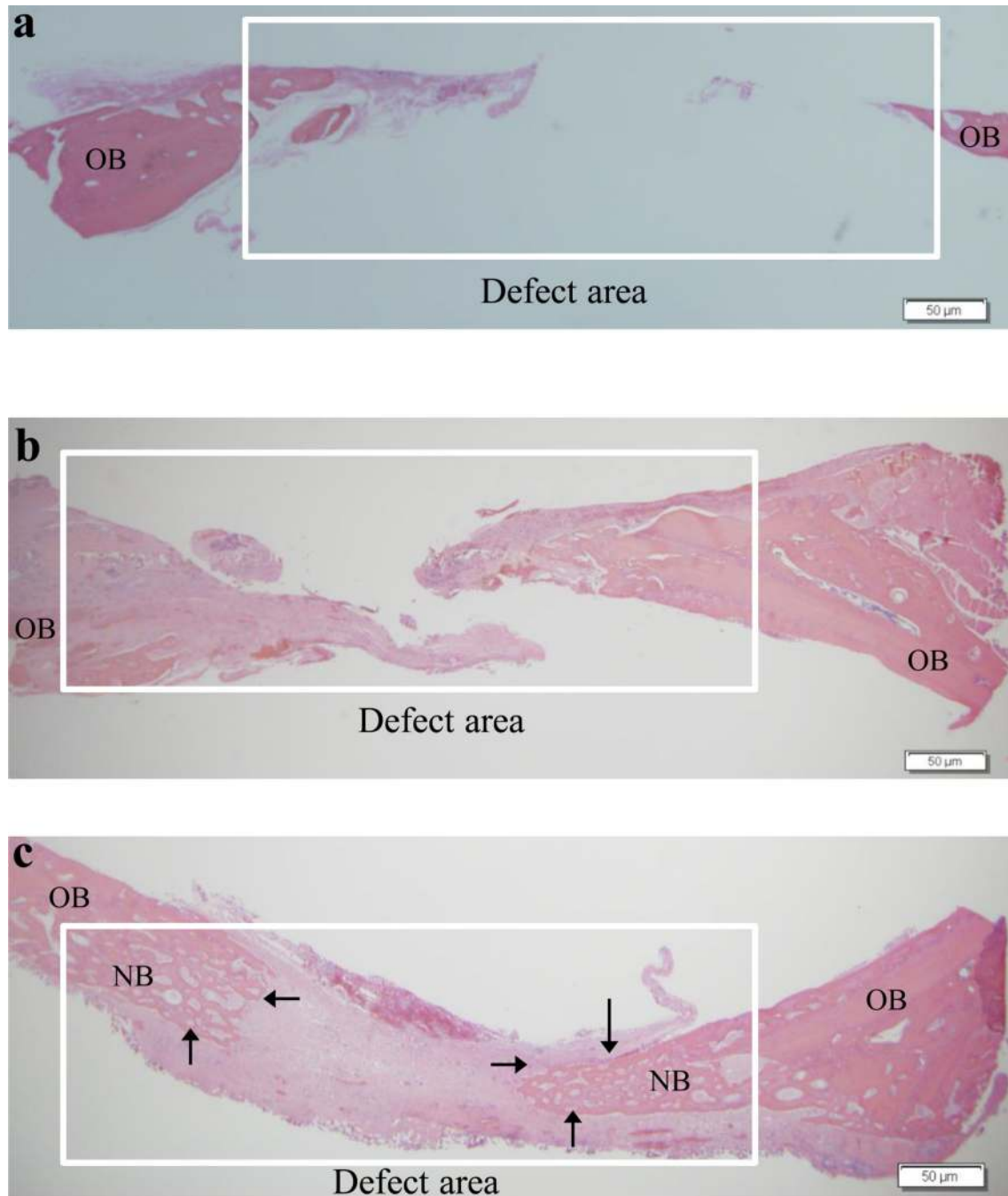


**Fig. 4.** Representative histology sections demonstrating the extent of new bone formation in the defects at 4 weeks due to various treatments: empty defects (a), chitosan scaffolds (b) and copper-loaded chitosan scaffolds (c). OB = old bone and NB = new bone. Note the partial bridging of new bone in the copper-loaded chitosan test group indicated by the arrows. Scale bar, 50 μm.